

AD A032443

FC

6
ACOUSTICALLY SCANNED OPTICAL IMAGING DEVICES
12

9
Semiannual Report, No. 2
1 January - 30 June 1976

15
Contract: N00014-76-C-0129 add
ARPA Order No. -2778
Program Code No. 4D10

Scientific Officer:

Dr. David K. Ferry
Director Electronic and
Solid State Sciences Program
Physical Sciences Division
Office of Naval Research
Department of the Navy
800 North Quincy Street
Arlington, Virginia 22217

14
GH-2616

G. L. Report No. 2616 ✓

11
September 1976

12
47p.

10
Gordon S. Kino
Principal Investigator
(415) 497-0205

D D C
RECEIVED
NOV 24 1976
D

DISTRIBUTION STATEMENT A
Approved for public release;
Distribution Unlimited

Sponsored by

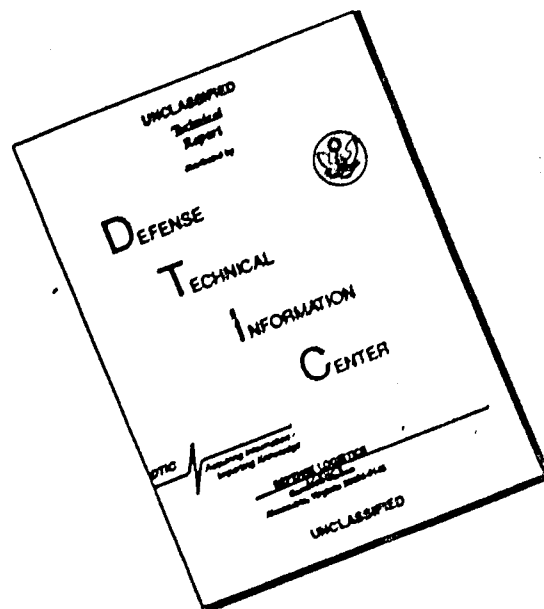
Advanced Research Projects Agency

ARPA Order No. 2778

Ginzton Laboratory ✓
W. W. Hansen Laboratories of Physics
Stanford University
Stanford, California

409640
LB

DISCLAIMER NOTICE



THIS DOCUMENT IS BEST QUALITY AVAILABLE. THE COPY FURNISHED TO DTIC CONTAINED A SIGNIFICANT NUMBER OF PAGES WHICH DO NOT REPRODUCE LEGIBLY.

D D C
RECEIVED
NOV 24 1976
D

ACOUSTICALLY SCANNED OPTICAL IMAGING DEVICES

SUMMARY

A reliable and simple airgap convolver constructional technique using rail supports has been devised and tested. An array of v groove isolated mesa p-n diodes has been fabricated in silicon. This gives excellent isolation between the diodes. The results obtained on convolvers and optical imaging devices are in excellent agreement with the theory that ^{has been} ~~we have~~ developed.

We have demonstrated the use of these devices as storage correlators. With these correlators, we have been able to correlate FM chirp signals with a time-bandwidth product of 90. In one experiment, we have shown how such devices may be used to correct system errors in radar and sonar systems by storing a reference echo distorted by the system, and correlating it with a later echo distorted in the same way.

We have demonstrated various kinds of optical image processing. But, we believe that most of these experiments are superceded by early results we have obtained using the storage devices as optically sensitive imaging devices, This principle involves changing the effective storage time in the presence of light. Sensitivities of the order of $0.1 \mu\text{W}/\text{cm}^2$ with good dynamic range have been measured. We would expect to obtain a dynamic range of 50 - 60 dB eventually.

We can now make reliable reproducible ZnO on Si convolvers. Our aim is to make ZnO on Si storage correlators and imaging devices. This requires improvements in the silicon p-n junction technology which we are able to test more quickly in the airgap devices.

SEARCHED	INDEXED
SERIALIZED	FILED
NOV 24 1976	
FBI - MEMPHIS	
REX H. ON FILE	
STABILITY 0000	
SERIAL	

DISTRIBUTION STATEMENT A
Approved for public release;
Distribution Unlimited

ACOUSTICALLY SCANNED OPTICAL IMAGING DEVICES

I. INTRODUCTION

During the last six months, we have continued the parallel development of both the airgap and ZnO on Si convolver technologies. Our long term goal is to demonstrate the value of these devices for performing both signal processing and imaging.

During the past six months, experiments on optical imaging and convolvers has been carried out on this contract, as well as our work on a stable airgap and ZnO on Si technology. However, initial tests on storage devices were carried out with Joint Services and NSF support. We have used the same developments in the convolver technology to demonstrate all the devices; the optical imager, the convolvers, and the acoustic surface wave storage correlators. We report the storage results here also, as they are a direct outcome of the technological developments carried out on this contract and would not have been possible without this work, and because the use of the storage principle has enabled us to demonstrate a very large improvement in sensitivity and dynamic range of the optical imaging device.

We have made major strides in the development of the airgap convolver technology, and have developed a rail supporting system, which is stable and uniform. This, we believe, is a relatively simple airgap convolver system with all the advantages of the post supported system developed by Lincoln Laboratories, but with much simpler masks, which makes a system that is far easier to keep dust free during assembly; normally a major problem.

Employing this airgap technology, we have demonstrated an airgap p-n junction storage convolver. With this device we have been able to characterize in detail the optical imaging sensitivity, and the convolution efficiency, and have begun to develop a detailed theory of storage processing. We have demonstrated various important signal processing functions, including, chirp transforms of optical images, slow scans, and good optical resolution ($89 \mu\text{m}$). With the storage devices, we have demonstrated chirp signal compressions, Barker code correlation, and pulse expansion. With the chirp compression technique, we have demonstrated how the storage convolver can significantly improve the performance of an acoustic pulse echo system, by removing the distortions in the echo generated by errors in the system itself.

Because of the ease in replacing the silicon in our airgap storage correlator, we have used this device as part of an intensive program to develop the silicon technology needed for diode convolvers, storage correlators, and imaging devices. The best of these arrays are being used, where applicable, in the program to develop a ZnO on Si storage convolver. We have found this to be a much faster approach than the direct development of the silicon technology in the ZnO on Si devices, because there are so many steps in making such a device that it is not always obvious which step has influenced the final result. Furthermore, with the large number of steps involved in fabrication, it is far more difficult to vary parameters of interest in a controlled fashion.

The AnO convolver program has proceeded in two ways. First, we have improved the process technology, and, as a result, the device yield.

Secondly, we have tested some of our diode storage arrays in ZnO devices, evaluating Schottky diodes, and p-n junctions with both metal and polysilicon overlayers. We have demonstrated good optical sensitivity and storage effects, but only poor definition, so far. As we have already stated, convolver technology is directly applicable to storage correlation devices. As a signal processing device, the storage correlator can carry out functions which are extremely difficult to duplicate in other devices. It gives a major improvement in flexibility over earlier ASW convolver devices, because it does not require synchronized inputs. It directly performs either convolution or correlation, and it has the capability of integrating signals.

An important application of this principle is to imaging. We have made initial demonstrations that the storage convolver offers very high and controllable sensitivity, and a high dynamic range. It allows the processing of images with much less difficulty as compared to convolvers with no storage, used as imaging devices. Thus, we regard the development of this relatively new storage convolver technology as being vital to both image processing and signal processing using acoustic surface waves. We, therefore, have placed, and intend to place major emphasis on this mode of operation and the technology required for it.

II. PRESENT STATUS

A. Airgap Convolver

1. Construction Techniques

Approximately one year ago we began developing an airgap structure with good enough efficiency and uniformity to perform high quality imaging and signal processing, yet with enough simplicity to allow quick replacement of the silicon. Some of the results of this work have been described in the last progress report, and in detail in a report by R. Joly,¹ and in a paper submitted to and accepted by Applied Physics Letters, which forms part of the Appendix. In this structure, the silicon is separated from the LiNbO_3 by a set of seven parallel $4 \mu\text{m}$ wide spacer rails which have been rf sputter etched into the LiNbO_3 . This is a simpler configuration; and the processing, which uses rf sputtering, rather than etching, is cheaper and simpler than that for post supported devices. The narrow rail configuration is illustrated in Fig. 1(c) and compared to the post supported and earlier SiO_2 rail structures illustrated in Fig. 1(b) and Fig. 1(a), respectively. The convolver structure shown in Fig. 2 can be dipped in acid to remove dirt just before assembly, and is then mounted in a small brass package for rf isolation, as shown in Fig. 3.

A further improvement has been obtained by fabricating an array of v-groove isolated p-n junction diodes in the silicon. Convolution occurs through modulation of the diodes' space charge layer widths by the signals. An important advantage here is that each nonlinear element is isolated from the next, which eliminates sideways carrier diffusion effects. This allows very high resolution imaging, or storage

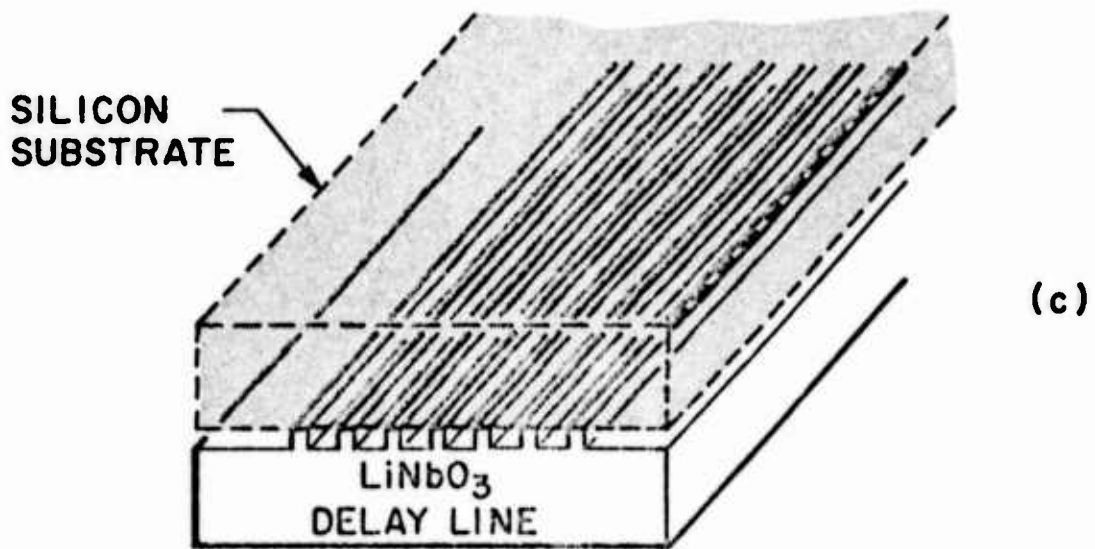
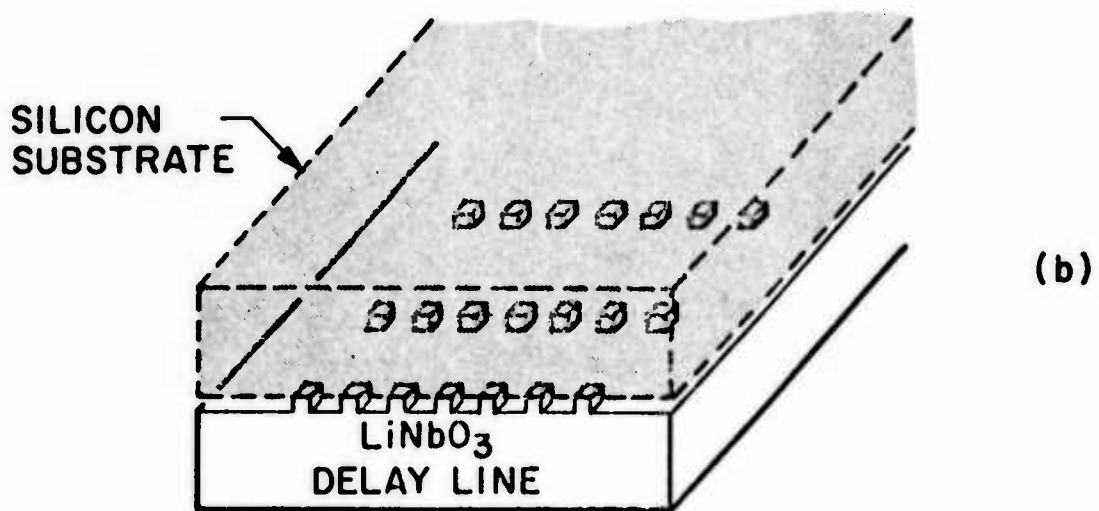
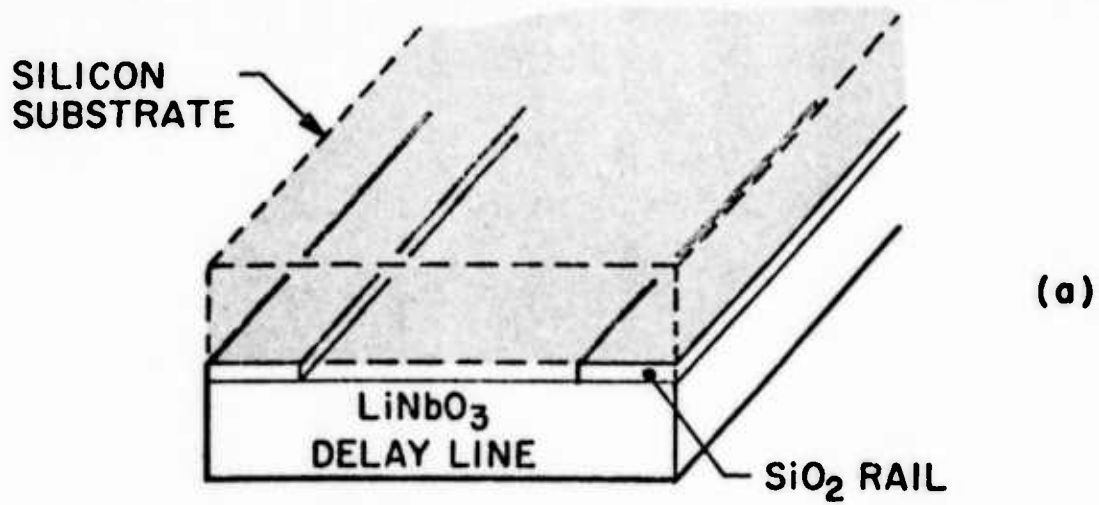


FIG. 1 - Airgap Convolver (a) configuration with SiO₂ rails
 (b) configuration with posts (MIT)
 (c) configuration with narrow rails

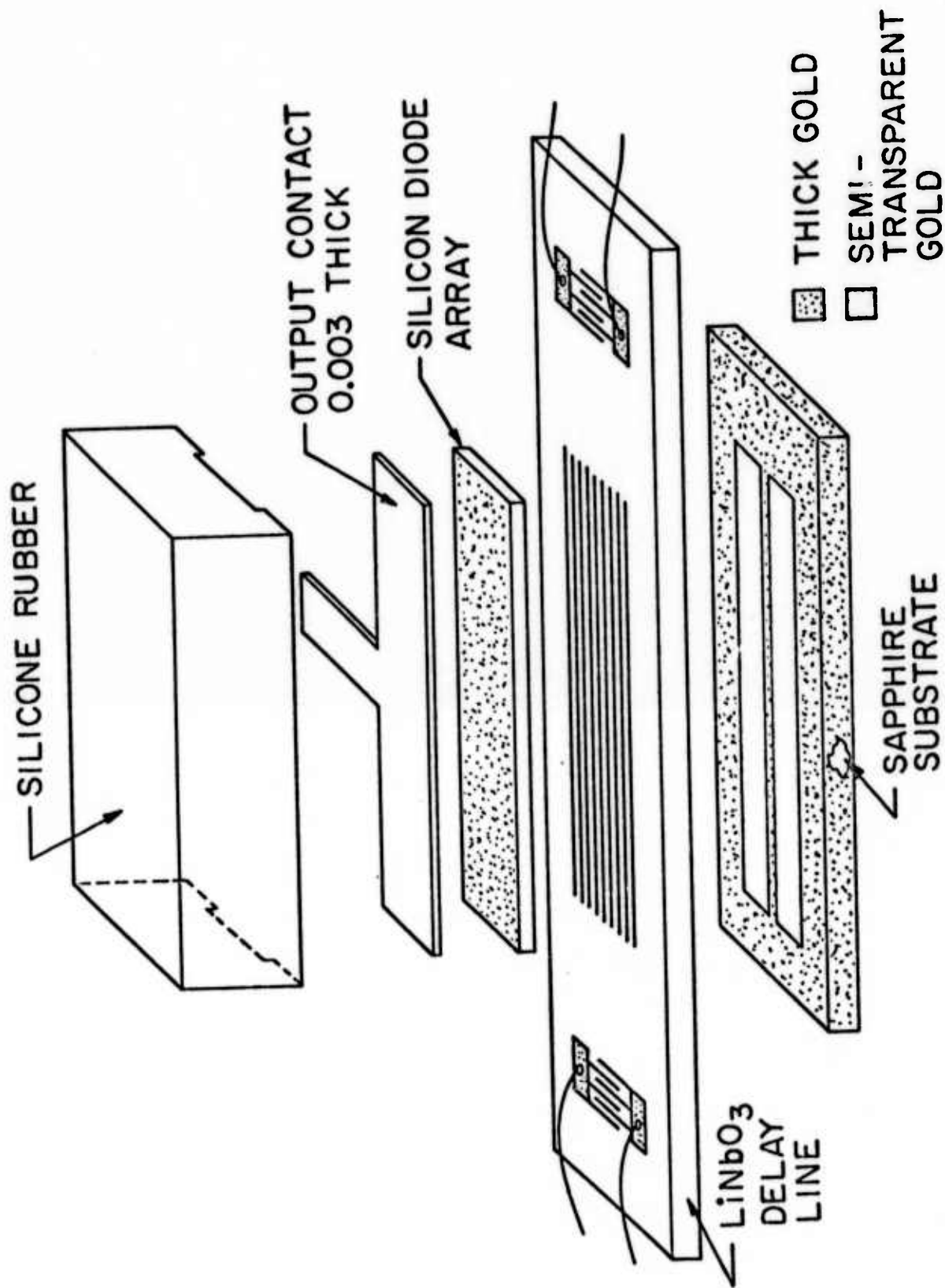


FIG. 2 Convolver exploded view

CONVOLVER
CARRIER

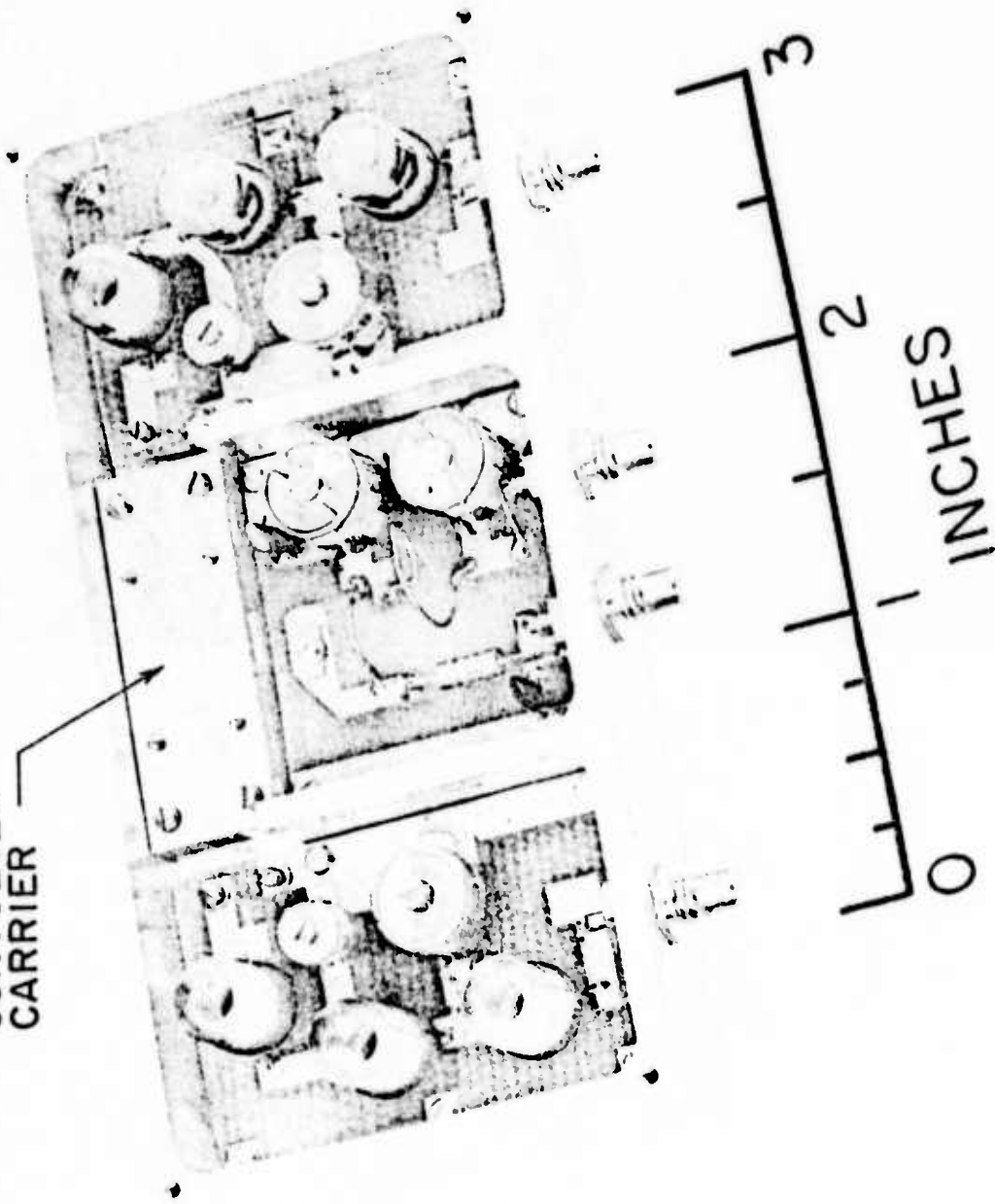


FIG. 3 - Complete convolver

of a signal whose wavelength on the LiNbO_3 is as short as two diode lengths (for our device this is $16 \mu\text{m}$, or 200 MHz).

The basic technology for making such diodes is very simple. It involves diffusing a p^+ layer into the n-type material, then etching grooves into the substrate so as to form separate diodes. $\langle 100 \rangle$ silicon is required for a 45° groove, for etching is very slow in the (111) direction. On the other hand, deep rectangular grooves can be etched in (111) material, and diode arrays can be made this way, as we have also illustrated.

It should be pointed out that we have also devoted considerable attention, before and after arriving at this groove configuration, to making simple multiple diode arrays with p^+ layers diffused in through windows in SiO_2 . With $4 \mu\text{m}$ spacing on nominally $4 \mu\text{m}$ wide diodes (actually $5 - 6 \mu\text{m}$, after sideways diffusion), the depletion layers of the diodes tend to merge. But whether this occurs or not is somewhat dependent on the applied dc fields and whether the surface between the diodes is oxidized, leading to a positive surface potential, or is bare, leading to a depleted surface. With an oxidized surface, some isolation between the diodes is observed, but it is not as good as with the mesa diode. Difficulties can also be encountered with inversion layers formed near the edge of a diode. These are normally eliminated in a vidicon structure by the use of metal electrodes of larger area than the diode in contact with the p^+ layer.

2. Operation as an Airgap Convolver

We reported on our results with p-n diode arrays in the last

progress report. Here we shall give a short summary of the convolver results obtained with the mesa diode arrays.

These arrays have proved to be more uniform than the equivalent diffused diode arrays. The uniformity of the response of such a convolver is measured by convolving a narrow pulse against a long pulse, as shown in Fig. 4. It will be seen that the uniformity along the length of the structure is of the order of 1.5 dB. Depending on the material used, the measured convolution efficiency has varied from 52 dBm to 58 dBm, and is usually within 1 dB of the predictions of the theory developed by Joly. A curve of output power versus input power of a device with a 1500 Å airgap is shown in Fig. 5. As the noise figure of the output circuit is ~ 90 dBm, it will be seen that the dynamic range of the convolver to the 3 dB compression point is over 60 dB.

3. Operation of a Convolver as an Optical Detector, without the Use of Storage

The convolver has been used to detect light directly by its effect on the optical output. A detailed theory of this mode of operation has been developed.^{1,2} (see Appendix) This theory predicts that, when a p-n junction is illuminated, electrons and holes are generated and the diode becomes forward biased, so that the forward current I_F is equal to the current generated by the light. Thus, the diode acts as a photovoltaic detector whose depletion layer thickness decreases, and capacity increases with illumination. As the convolver output is proportional to dC/dV where C is the diode capacity, V , the voltage across it; the convolver output increases initially with illumination. With very intense light, the conduction current in the diode loads the diode, and the output decreases.

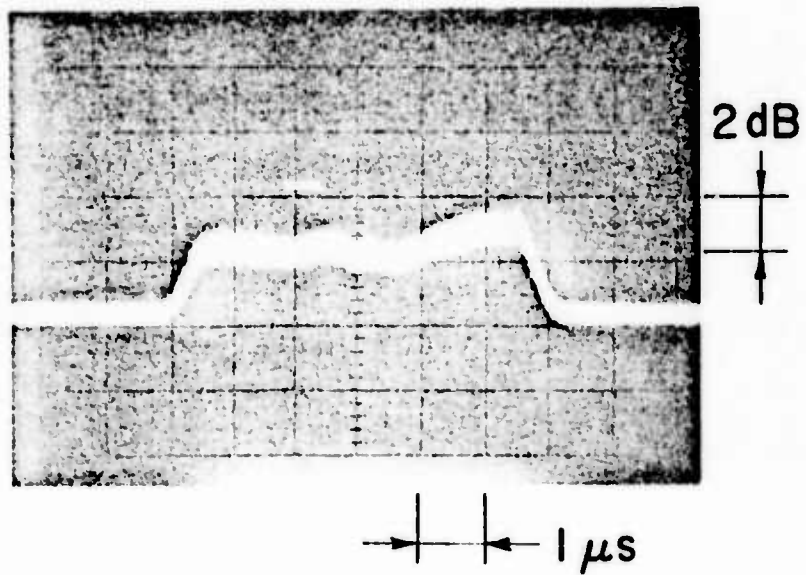


FIG. 4 - Interaction region uniformity;
 mesa structure,
 1500 \AA airgap,
 $F_T = -58 \text{ dBm}$,
 $\Delta F_T = 1.5 \text{ dB}$.

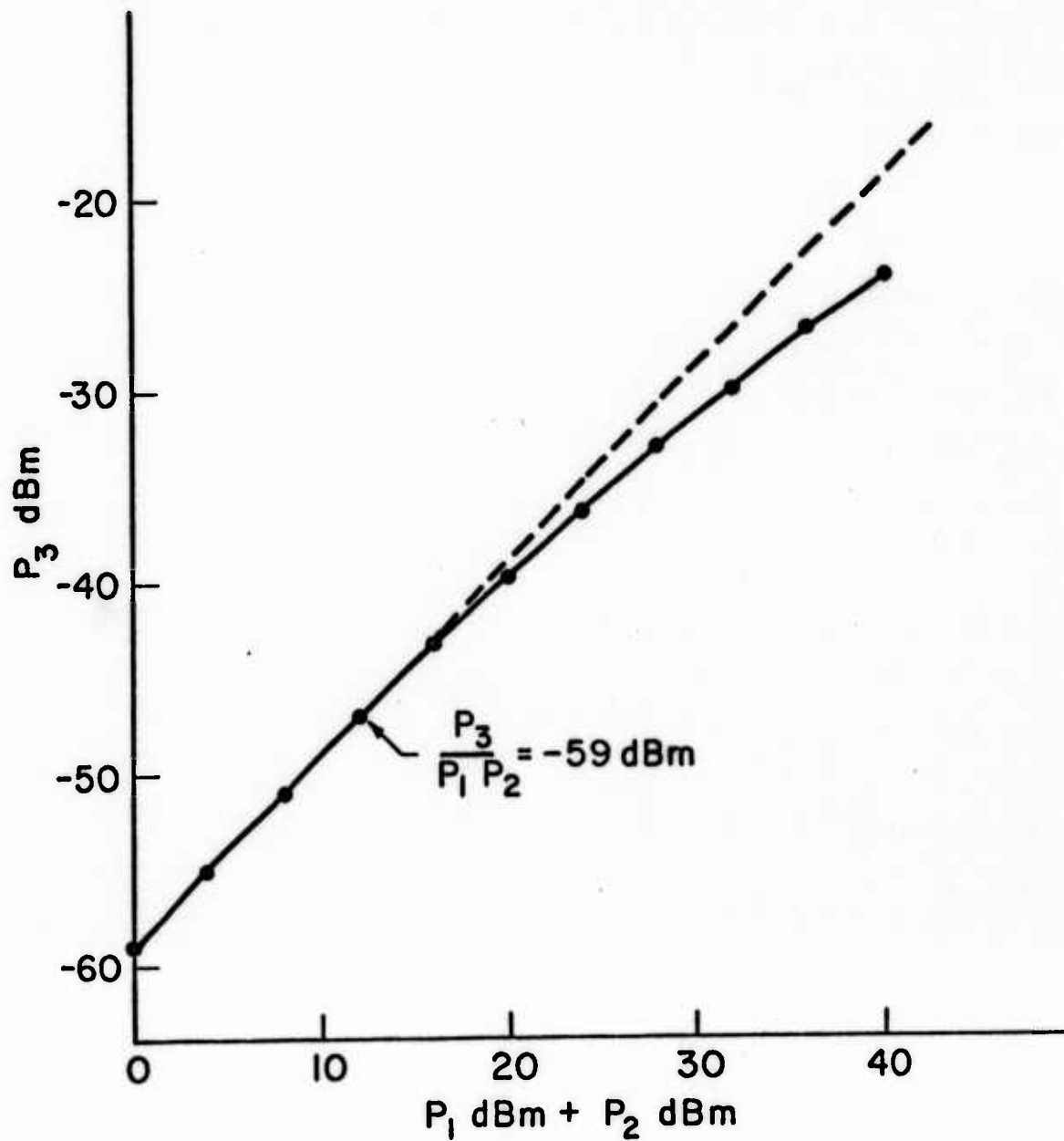


FIG. 5 - Output power versus input power;
 mesa structure,
 1500 Å airgap.

In practice, the measured change in output of an airgap convolver is of the order of 2 - 3 dB, as the light intensity is changed. The results, described in the Joly report, are in good agreement with theory, but indicate a very limited dynamic range without further measures being taken. These involve the use of Fourier transform techniques or a grating placed in front of the device to give spatial filtering. By far the most important technique which will supercede the others, in our opinion, is the use of storage methods to yield high dynamic range and sensitivity.

The first method involves taking the Fourier transform of the optical image first by feeding two chirp signals of opposite chirp slopes, but centered at the same frequency, into the two convolver inputs, and then gating the convolver output properly. Since the dark signal is contributed uniformly by the whole length of the interaction region of the convolver, it will appear as the zero spatial frequency component, i.e., the zero time component, of the spatial Fourier transform.¹ So, by gating the output signal properly in time, this component can be removed. Such demonstrations are described in the report by Joly. They have only yielded a 20 dB dynamic range, due to the effect of small nonuniformities in the system which yields dark current components with finite or spatial frequencies.¹

The second technique, which we have described before,^{3,4} involves the use of a periodic grating and two chirp signals with their center frequencies, ω_1 , ω_2 , respectively, being offset by an amount determined by the periodicity l of the grating, such that $(\omega_1 - \omega_2)l/v = 2\pi$, where v is the acoustic velocity. Now the dark signal has a different spatial frequency from that of the light, and can be eliminated.

This nondegenerate mode of operation of the convolver in optical imaging applications had already been demonstrated in this laboratory by Gautier.^{3,4} However, in his experiment, he focused a coarse periodic grating on the silicon surface through the LiNbO_3 delay line. Due to many difficulties encountered in alignment, in focusing, and in generating the right chirp signals, his experiment was difficult to set up. So finding the optimum operational conditions was extremely tedious. In order to overcome these problems, a fine periodic grating with a periodicity of 89μ is pressed against the bottom surface of the LiNbO_3 substrate. With the convolver used in this experiment, it was found necessary to place a metal gasket between the grating and the LiNbO_3 substrate. The purpose of the metal gasket is to physically separate the grating from the LiNbO_3 substrate, since we found in our earlier experiments that the effect of the periodic grating is somehow felt by the silicon surface, even in the dark, and thus a strong dark output signal is still present. This effect is real, but one which we have found difficult to explain.

For our experiment, we used a convolver with an airgap of 1500 \AA , and the two input transducers are centered at 100 MHz and 140 MHz, respectively. The p-n junction diode array used is of the v-groove mesa type, as already described. We also used the matching networks for the input transducers described in our last progress report. We were able to obtain Fourier transforms in this system with a dynamic range of 30 dB.

We concluded that the p-n mesa diode configuration gives good isolation because we can detect light with a spatial frequency of $89 \mu\text{m}$.

In our storage experiments, the detected spatial frequencies are, in fact, of the order of $15 \mu\text{m}$. But, it is apparent that, although we can obtain and have obtained spatial transforms of optical images with approximately 180 spots (30 MHz bandwidth, 6 μsec long, reformed in a dispersive delay line of 2.5 MHz bandwidth 120 μsec long), the dynamic range and sensitivity is still badly limited by the loss of light in the grating, which is approximately 14 dB. This is because half the light is attenuated and only one spatial harmonic is used in the detector. As the storage experiments were so encouraging, yielding far better sensitivity and dynamic range on the first try, we decided to abandon these experiments and devote all our efforts to employment of this storage phenomenon.

4. Storage Correlation in the Airgap Convolver

Because of the good interdiode isolation found in the v-groove array structure, our convolver functions well as a storage correlator as well as an imaging device. We, therefore, have demonstrated it in this mode of operation, because of the great potential importance of this signal processing technique, and, as we have shown, as an optical imaging device.

Several modes of storage correlator operation are possible. In one case, a charge pattern is written into the diode array through the nonlinear interaction of an rf signal $F(t)$ applied to the diode array top plate (T) and the electric fields associated with a short acoustic pulse injected on the interdigital transducer (L) which travels along the delay line, as illustrated schematically in Fig. 6. After the

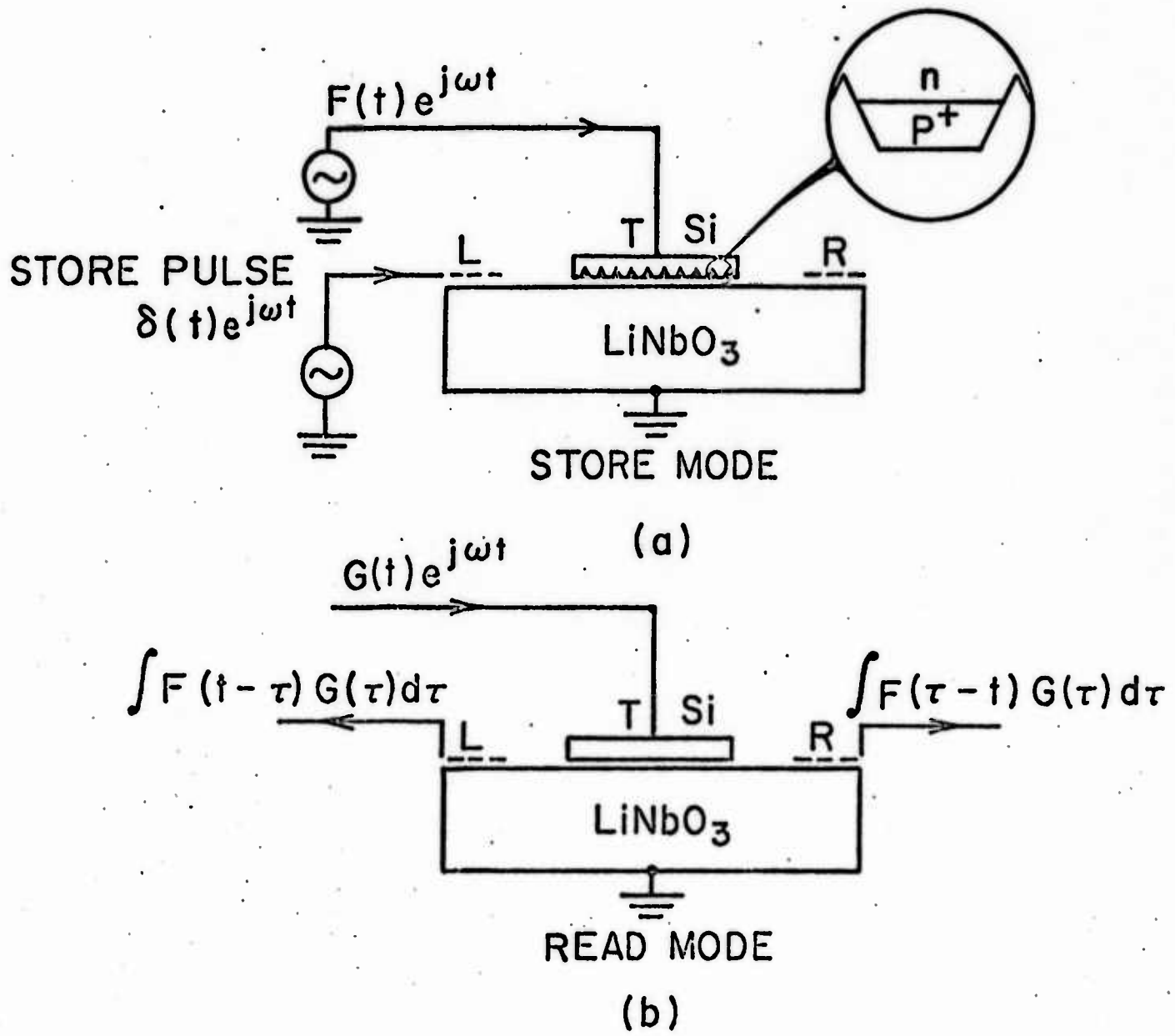


Fig. 6. Storage Correlation in the Airgap Convolver.

storage interval, by applying an rf signal ($G(t)$) to the top plate (T), the convolution of this signal with the stored signal is obtained at the original input port, and the correlation of the two signals at the other acoustic port. In the present case, one transducer is used for a short input storage pulse, and the other for readout. In general, the output will be the correlation of the second top plate input signal and the stored signal. Alternatively, we can apply the pulse to the array top plate (T) and the signal $F(t)$ to one of the transducers, and can read out from the top plate T by inserting the reading signal $G(t)$ on one of the transducers L or R. The output will be the convolution or correlation of $F(t)$ and $G(t)$.

In our experiments, the first mode of operation has been used. The principle reason is that this scheme provides good isolation between the top plate and output port R .

We have characterized the storage process in our own airgap p-n junction storage correlator. The storage half-height time is 8 msec. The diodes take only one or two nanoseconds to charge.

Summarizing the general properties, typical input levels are 25 dBm at the acoustic port and 60 V p-p at 98 MHz between the silicon and ground. The top plate is matched to provide better than 20 MHz bandwidth. The transducer bandwidth is 38 MHz. These characteristics have allowed us to perform a number of interesting signal processing experiments. In one of these, a 50 μ sec pulse was inserted on the left hand transducer and used to store a 15 MHz bandwidth, 6 μ sec long

linear FM chirp inserted on the top plate. The correlation of this stored chirp was taken with a second identical FM chirp. The measured compression ratio was 75 , compared to the theoretical value of 90 . More details of this experiment are given in the paper in the Appendix.

It is significant to note that, for this experiment to succeed, the diode array must store not only the amplitude, but also the phase of the $98 \text{ MHz} \pm 15 \text{ MHz}$ chirps. This means that, while the diodes are dense enough to meet the requisite sampling criterion (2 per wavelength are required, we have 4), they are completely decoupled from one another electrically. The chirp correlation experiment performs the dual purpose of demonstrating the power of the storage correlator as a signal processing device and its applicability in evaluating the performance of diode storage and imaging.

We have also used this device to correlate 3 and 5 bit Barker codes. The principal difficulty in this and other more sophisticated applications to be described is that, in these experiments, there was some feedthrough of the reading signal to the output port. Thus, although the reading signal can be varied over a 50 dB range, both the correlation output and the feed through signal vary in amplitude together, and the stored output is only 10-20 dBs above the feed through signal. It has not, therefore, been possible to store very long codes, and measure their sidelobe levels.

We have eliminated capacitive feedthrough of these signals by careful shielding. The rest of the feedthrough is due to bulk waves, and surface wave excitation at the ends of the silicon. We are taking steps

to eliminate these effects, and are quite confident that we will be able to obtain a 50-60 dB dynamic range, for the output is comparable to that of the device operated as a convolver.

One of the principal applications of the storage correlator is, we believe, to correct for these distortions in sonar and acoustic systems suitable for nondestructive testing.

As described in the accompanying paper in the Appendix,⁵ we have made such a demonstration. We used an acoustic transducer in water, excited by a 2.5 MHz wide chirp with a center frequency of 3.5 MHz. The acoustic beam was reflected from a piece of plastic, and, after mixing, up to 98 MHz was stored in a storage correlator. A later echo was then correlated with the stored chirp. A narrow correlation peak was observed even when a transducer with a very poor phase response, and hence, transient response was employed. (see Appendix) This is typically because both the reference and the second echo are distorted in the same way.

The principle can also be applied to radar systems, to pattern recognition, and to imaging systems. If a transmitted signal is distorted by the antenna or through propagation along a distorting path, it can be corrected by using a reference echo near the object of interest, or on the object itself. Alternatively, in a communication system, a pulse can be sent through the communication channel, which may distort it. If this distorted pulse is stored in the storage correlator at the receiver, an unknown signal passing along the same path can be correlated with the stored pulse, and the distortion in the system corrected.

Finally, we have demonstrated the ability to perform pulse expansion.

Here, a double pulse was stored in the system. It was then read out with a slow chirp four times longer than the acoustic time length of the diode array. The output obtained was the Fourier transform of the stored pattern. Using a dispersive delay line matched to the readout chirp, the output was retransformed, yielding a pulse expanded in time by a factor of 4.

The significance of this and similar experiments is that the storage convolver's time-bandwidth product need not be limited only by the length of the input signals, because the p-n junctions can integrate the charge. These input signals can be quite long. This raises the possibility of demonstrating a convolver with a time bandwidth product of several thousand.

5. Optical Imaging with the Storage Correlator

In addition to the signal processing applications, the storage convolver promises to be of great value in imaging work. We have made preliminary tests of its light sensitivity employing the same system as in the pulse expansion experiment described earlier. A pulse as long as the entire array is stored; wherever light hits the array, it generates carriers in the diode depletion regions. These carriers discharge the diodes locally through recombination with the stored charge. Thus, wherever light shines on the array, the readout amplitude will be reduced. Because the device integrates from the readin to readout time, the sensitivity is variable, and the signal to noise ratio is high. In this first experiment, a 50 mW/cm^2 source (bright incandescent lamp) reduced readout 15 dB after 100 μsec delay. A $3 \mu\text{W/cm}^2$ source (fluorescent lights) reduced readout 10 dB after a 7 msec delay. Thus, the storage correlator exhibits better imaging sensitivity than the best convolvers.

Basically, the device acts as if a spatial filter has been read into it. The dynamic range will be dictated only by the dynamic range of the reading system. Thus, we would expect to obtain 50-60 dB dynamic range in the output, and very much greater sensitivity than that which we have already observed. These results correlate well with the far more complete ones of this type obtained in France at about the same time (April 1976). It is apparent that the device is capable of becoming an extremely sensitive optical imaging and transform system.

B. ZnO on Si Device and p-n Junction Arrays

As mentioned in the Summary, we are pursuing the development of a ZnO on Si storage correlator. Because this work proceeds parallel to our airgap convolver program, and, because we have the facilities at the Stanford Integrated Circuit Laboratory at our disposal, we have fabricated a number of planar diode storage arrays and evaluated them on the airgap device, before proceeding with the construction of the more intricate ZnO on Si devices. This work has also given us a much better understanding of the physical processes and problems associated with the storage correlator.

In order for a storage or optical imaging array to work satisfactorily, there must be a high degree of isolation between adjacent diodes. Since the airgap device works at 100 MHz, there is a significant difference in stored charge between any two adjacent diodes, and, unless the isolation is satisfactory, no readout amplitude will be observed. When we employed a p-n junction diode array with $4 \mu\text{m}$ wide diodes and $4 \mu\text{m}$ spaces on 15 $\Omega\text{-cm}$ material, no storage was observed. Most likely, this was because the diode depletion layers overlapped, allowing interdiode

electric fields to form and causing a current to flow between adjacent diodes. When the same diode array was v-groove etched, good storage performance was observed.

We then fabricated three types of arrays. All had 6 μm wide diodes with 12 μm interdiode spacing. In the first type, the diodes had 12 μm wide v-grooves, so each diode sat atop its own mesa. In the second type, 6 μm v-grooves were etched. This left some bulk material around each diode, but insulated them from any interdiode current flow. The third structure was planar, with no v-groove isolation. When tested on the airgap device, only the mesa structure gave any readout amplitude. This indicates an additional problem; the surface wave electric fields locally bias the diodes, causing them to discharge. Thus, the edges of the diodes must be protected from the surface wave electric fields, either by isolation etching or by overlay structure. Since isolation etching is not feasible in the monolithic ZnO on Si structure, the overlay structures were explored.

So far, we have evaluated a diode array in which a p^+ doped polysilicon layer is laid over the p-n diodes. Each polysilicon overlay has a width of 10 μm ; the spacing is 5 μm . The diodes are 5 μm wide with a 10 μm interdiode spacing. The storage efficiency of this array approaches that of the v-groove isolated arrays. We are also testing aluminum and gold overlay structures which should have an efficiency equivalent to the polysilicon arrays, but may enable the growth of higher quality ZnO.

The ZnO on Si convolver work has proceeded along two lines. First, we have greatly improved our fabrication techniques. Second, we have attempted to make a storage correlator using the diode arrays described earlier.

The fabrication efficiency has been aided by the development of a process that allows us to make up to eight device on a single wafer, separating the devices only as a final step. This keeps the process more controlled, each device is handled less, and the higher number of devices (earlier, four were made in each run) gives a higher yield of workable devices from each run.

The second improvement has been in the development of two bonding technologies. Earlier, hot wedge bonding was used. This would often crush the ZnO and short the bonding pad to the silicon. We are now able to make reliable bonds in two ways. We can make a cold wedge bond, which is fast but yields a weak bond. Stronger and very reliable bonds are provided using a silver epoxy conductive paste that sets upon the application of heat. With this technique, we can reliably make bonds that have less than $4 \mu\text{m}^2$ area and are stronger than the adhesion of the bonding pad to the ZnO.

One set of ZnO on Si storage correlators has been fabricated using the polysilicon overlay arrays. The insertion loss was low, 22 dB, indicating that the overlay structure does not cause serious loss due to acoustic reflections. No storage was obtained, however, because the quality of the ZnO over the polysilicon was low. This indicates that the use of a metal overlay structure may give better results, since gold and possibly aluminum can be deposited for properly oriented ZnO growth.

The ZnO project's most immediate aim is the demonstration of a ZnO on Si storage correlator. We are carrying out a series of tests to see if ZnO can be grown on sputtered or deposited on SiO_2 . Simultaneously, we are testing the metal overlay arrays. The first set of

experiments will allow us to grow good ZnO on any material, by interposing a thin layer of SiO₂. Coupling this with the results of our work with overlay diode array structures should allow us to fabricate a ZnO/Si monolithic storage correlator. Once we are able to fabricate such a device, we intent to duplicate as many of our airgap results as possible, both with signal processing and imaging in the storage mode.

REFERENCES:

- 1 - R. Joly, "Design of a Convolver for Optical Imaging," Ph.D. thesis G. L. Report 2560, Stanford University, Stanford, California, 1976.
- 2 - R. Joly, "A Mesa P-N Diode Array Acoustic Surface Wave Convolver," accepted for publication by Appl. Phys. Lett.
- 3 - G. S. Kino, "Acoustoelectric Interactions in Acoustic Surface Wave Devices," invited paper, Proc. IEEE, Special Issue on Surface Acoustic Wave Devices and Applications, 64, No. 5, pp. 724-748, May 1976.
- 4 - H. R. Gautier, "Acoustic Wave Semiconductor Convolver Applied to Electrical and Optical Signal Processing," Ph.D. thesis, M. L. Report 2448, Stanford University, Stanford, California, 1975.
see also:
H. R. Gautier and G. S. Kino, "A Detailed Theory of the Acoustic Wave Semiconductor Convolver," accepted for publication by IEEE Trans. on Sonics and Ultrasonics, 1976.
- 5 - P. G. Borden and G. S. Kino, "Correlation with the Storage Convolver," accepted for publication by Appl. Phys. Lett.

APPENDIX

A MESA P-N DIODE ARRAY ACOUSTIC SURFACE WAVE CONVOLVER

by

R. Joly

Preprint

G. L. Report No. 2585

June 1976

rev. August 1976

Contract N00014-76-C-0129

submitted to

Applied Physics Letters

Edward L. Ginzton Laboratory
W. W. Hansen Laboratories of Physics
Stanford University
Stanford, California

A MESA P-N DIODE ARRAY ACOUSTIC SURFACE WAVE CONVOLVER*

by

R. Joly
Stanford University
Stanford, California
94305

Abstract

A new type of airgap convolver has been constructed. It uses a mesa p-n diode array, instead of the usual silicon slab, and narrow rails for supporting the diode array. Several different modes of operation for imaging have been demonstrated with this device.

*This work was supported by the Advanced Research Projects Agency of the Department of Defense and was monitored by ONR under Contract No. N00014-75-C-0129.

A MESA P-N DIODE ARRAY ACOUSTIC SURFACE WAVE CONVOLVER

by

R. Joly
Stanford University
Stanford, Ca. 94305

We describe in this paper a modification of the acoustic surface wave convolver which uses an array of p-n mesa diodes laid down in silicon. This eliminates transverse diffusion of generated carriers between the individual diodes and, hence, makes it possible to obtain good resolution in optical imaging and storage devices. We also describe the use of $4 \mu\text{m}$ wide rails etched in the LiNbO_3 to support the silicon. This configuration is much simpler to make than the post configuration, and gives negligible mass loading with no reflections; it is easily reproducible and mechanically stable. This basic system has shown excellent optical sensitivity and has proven very useful for a storage correlator, as described in an accompanying paper.

The shortcomings of the continuous surface wave Si-airgap convolver^{1,2} used as an imaging device² are: 1) carriers generated by a spot of light diffuse laterally. This blooming effect reduces the number of resolvable spots; 2) if the silicon surface is depleted by an external bias, the generated carriers can be trapped in fast surface states, yielding good light sensitivity. However, there are unwanted storage effects in slow surface states, with time constants as long as several hours; 3) with the silicon surface at flat band, surface trapping is unimportant, but diffusion effects degrade the light sensitivity and modulation transfer function.

Closely related problems occur when continuous surface convolvers are employed as storage correlators.

The diode array described here separates the diodes by means of etched grooves. Otherwise, diffusion of the carriers along the surface must be prevented by the introduction of some type of potential barrier. In Schottky diode devices, this may occur automatically.³ In p-n diode vidicon structures, a metal overlay on each diode introduces the necessary potential barriers.⁴ Diode arrays with etched grooves have the following advantages for storage and imaging: 1) the nonlinear interactions take place only in the diode depletion layers, so the convolver is not very sensitive to surface effects; 2) the number of resolvable spots is limited by the number of diodes, not by diffusion effects; 3) the use of the photo-voltaic effect and long storage times in reverse bias diodes should result in good light sensitivity and storage times.

Fifteen 2 cm x 2 mm diode arrays are processed simultaneously on a 2" diameter, n-type, 0.1 - 0.9 Ω cm, $\langle 100 \rangle$ silicon wafer. The 4 μ m wide p⁺ - n type mesa diodes are fabricated by shallow boron diffusion ($\approx 0.5 \mu$ m) into a 5 μ m thick, 15 Ω cm, arsenic doped epi layer. Individual isolated mesa diodes are obtained by anisotropic etching of 4 μ m wide, 2.8 μ m deep "V" grooves, with a warm KOH solution (100°C - 33:67 by weight KOH:H₂O). The best results are obtained with unoxidized diode arrays.

Figure 1 shows three different ways of defining an airgap of the order of 1500 Å in a Si-LiNbO₃ convolver structure. In (a) the silicon substrate bends easily under slight pressure and can make contact with the delay line in the region where the acoustic beam propagates. In (b) the 4 μ m x 4 μ m posts are obtained by ion beam etching.⁵ In (c) 4 μ m wide rails, with 150 μ m spacing, are obtained by rf sputter etching; AZ1350J photoresist protects the rails during the sputter etching. The processing associated with this configuration is much simpler than that

corresponding to the post configuration. The rails are stronger than the posts and there is no risk of coherent reflection, since there is no longitudinal periodicity. Because the total rail area is very small compared to that of the acoustic beam, the measured mass loading is less than 1 dB over a 2 cm length. The mass loading experiment was carried out by using low loss slabs, such as glass and 0.01 Ω cm silicon, in place of the diode array.

Figure 2 shows how the different parts of the convolver package fit together. The gold plated sapphire substrate is used as a mechanical support and provides the ground underneath the delay line; it is polished on both sides and has a clear window on the hidden face to allow the light to enter the device. The uniformity of the airgap is checked by inspection of the interference pattern between the silicon and the delay line through the transparent sapphire. The silicon slab has no leads bonded to it, so it can be very easily handled and cleaned in strong chemicals, such as sulphuric acid and buffered hydrofluoric acid, just before assembly. This considerably eases the dust problem. The delay line itself, with its Cr-Au deposited transducers and 5 mil diameter gold wires, is unaffected by $H_2O_2-H_2SO_4$ cleaning to remove dust and organic contaminants.

All the parts shown in Fig. 2 are stacked in a completely independent, entirely shielded small carrier. The matching networks are outside the carrier, so as to allow testing of different devices without making new matching networks every time. The YZ cut $LiNbO_3$ delay line is 3.5 cm long, 3.5 mm wide, and 0.5 mm thick. The three finger pair transducers launch 1 mm wide acoustic beams at a 100 MHz center frequency.

The terminal to terminal loss between the transducers is 19 dB and the 3 dB bandwidth is 38 MHz. The p-n diode convolver exhibits an overall efficiency $F_T \equiv P_s/P_1P_2 \approx -59$ dBm, which is within 1 - 2 dB of our theoretical estimate; and a uniformity of better than 2 dB in output along its length.

The convolver can be represented by the approximate equivalent input and output circuits shown in Fig. 3. In Fig. 3a, ϕ_{a1} and ϕ_{a2} are the rf potentials associated with the two input acoustic surface waves at the surface of the piezoelectric material, C_g is the gap capacity, r is the series resistance of the diode, R is the small signal rf dynamic shunt resistance of the diode, and $C(V)$ is the diode depletion capacity when the forward bias across it is V . In Fig. 3b, C_1 is the capacity of the diode to the output electrode, R_2 the series resistance of the output circuit, and C_2 the shunt capacity of the output electrode to ground.

The distributed diode output signal is, in first approximation, proportional to $\partial C/\partial V$. Under light illumination, each diode is forward biased by a current generator $I_0 = qG$, where G is the generation rate of carriers by light. As $\partial C/\partial V$ increases with the forward bias, and the diode is forward biased when it is illuminated, the output signal from an illuminated diode is higher than in the dark. So the device is basically a photovoltaic detector.

The output voltage increase is reduced by two loss mechanisms: 1) as the light intensity increases, the diode capacitance $C(V_0)$ increases. More rf current flows in the diode series resistance r , and the resistive loss increases; 2) as the light intensity increases further, the

diode dynamic resistance $R(V_0)$ becomes smaller and smaller, and the corresponding loss increases very rapidly. The loss due to $R(V_0)$ is only of importance for very strong light intensity of the order of $10^5 \mu\text{W}/\text{cm}^2$, for which $V_0 \approx 0.5 - 0.6$ volt. In our devices, the efficiency increases by 0.5 dB for a light intensity less than $1 \mu\text{W}/\text{cm}^2$, by 1.5 dB for $50 \mu\text{W}/\text{cm}^2$, and by approximately 2.5 dB for $10^4 \mu\text{W}/\text{cm}^2$. The dynamic range of the device in this form is limited. Several methods are available for improving the dynamic range and have been demonstrated by us.

The first method involves the use of an optical grating placed on the backside of the LiNbO_3 so as to give the image a spatial periodicity. By working with input signals at 100 MHz and 140 MHz, which difference in ASW propagation constants correspond to the spatial periodicity of the grating (87 μm), an output is obtained only when light is present. The measured dynamic range in this case is approximately 35 dBs.

A second alternative is to operate the device in a storage mode, and affect the storage time by illuminating it. Illumination will strongly diminish the storage signal readout. By this means, we have demonstrated noise limited sensitivities of the order of $0.1 \mu\text{W}/\text{cm}^2$.⁶

The third method is the use of Fourier transform techniques with two rf input chirps of opposite sign inserted in each transducer, as described by the author earlier. The output obtained is now the Fourier transform of the spatial response of the system. Frequency corresponds to spatial distance along the semiconductor, and time to the spatial frequency in the image. By gating the output at a particular time corresponding to a small spatial frequency, the dark signal can be decreased

and a dynamic range of 20 - 30 dBs obtained. In this case, the device uniformity and multiple reflections limit the dynamic range.

In conclusion, we have demonstrated a new type of airgap acoustic surface wave semiconductor convolver using mesa diodes on Si supported by narrow rails; it has excellent light sensitivity with an efficiency comparable to a good uniform airgap convolver. The efficiency is independent of any dc voltage applied to the diode array, as it should be. There is no hysteresis effect and no storage effects in surface states. Good response to light with an $80 \mu\text{m}$ spatial periodicity is obtained, so transverse diffusion in a mesa diode structure does not appear to be a problem. We would expect that, as the spatial period of the junctions is $8 \mu\text{m}$, the MTF would remain unchanged until the periodicity reaches this level.

ACKNOWLEDGEMENT

The author would like to thank G. S. Kino for his guidance and supervision, and H. C. Tuan, who carried out the measurement of dynamic range with the device illuminated through an optical grating. I would also like to thank H. Gautier for informing us of his results before publication.

FIGURES

Fig. 1. Methods of defining the convolver air gap:

- (a) SiO_2 rails
- (b) posts
- (c) narrow rails

Fig. 2. The convolver package assembly.

Fig. 3. Convolver equivalent circuits:

- (a) input
- (b) output

REFERENCES

1. N. J. Moll, O. W. Otto, and C. F. Quate, J. de Physique, 32, Colloque C-6, Supplement, pp. 231-234 (November-December 1972).
2. H. Gautier, G. S. Kino, and H. J. Shaw, 1974 IEEE Ultrasonics Symposium Proceedings, pp. 99-103 (1974).
3. K. A. Ingebrigtsen, R. A. Cohen, and R. W. Mountain, Appl. Phys. Lett., 26, p. 596 (1975).
4. C. Maerfeld, Ph. Defranould, and P. Tournois, Appl. Phys. Lett., 27, pp. 577-578 (1975).
5. H. I. Smith, 1975 IEEE Ultrasonics Symposium Proceedings, p. 238 (1975).
6. Ph. Defranould, H. Gautier, and C. Maerfeld, Appl. Phys. Lett., 29, pp. 79-81 (1976).

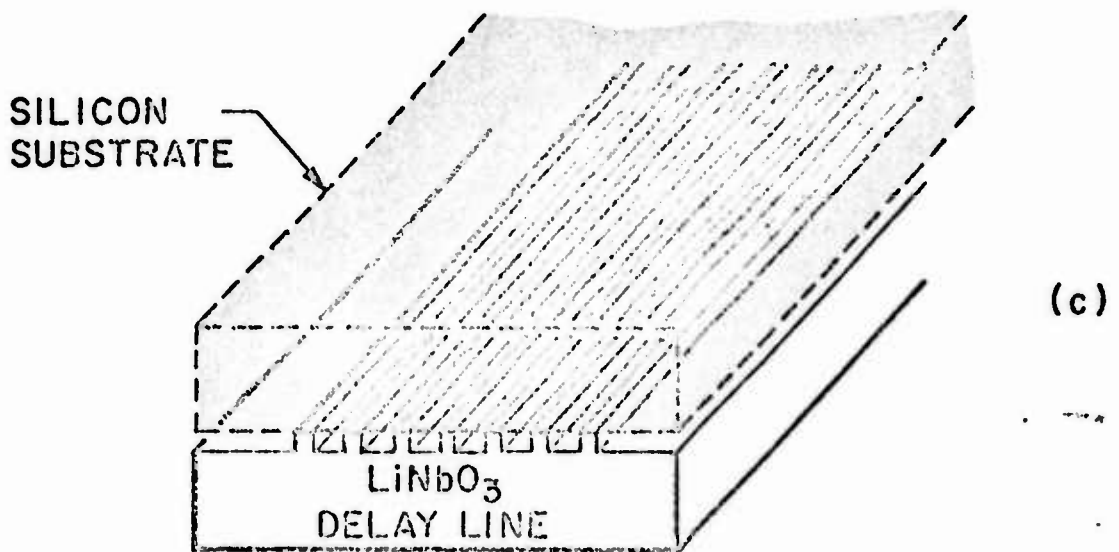
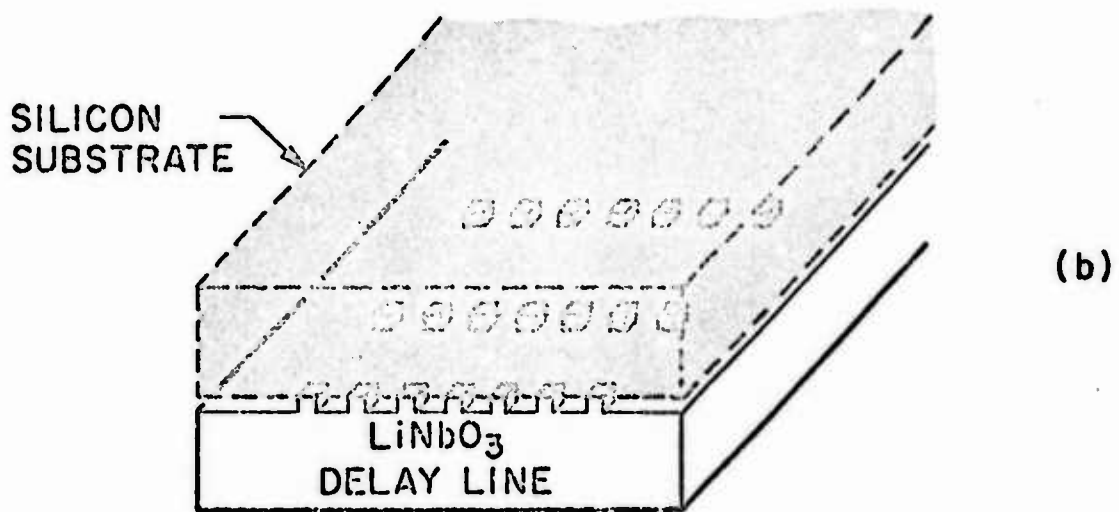
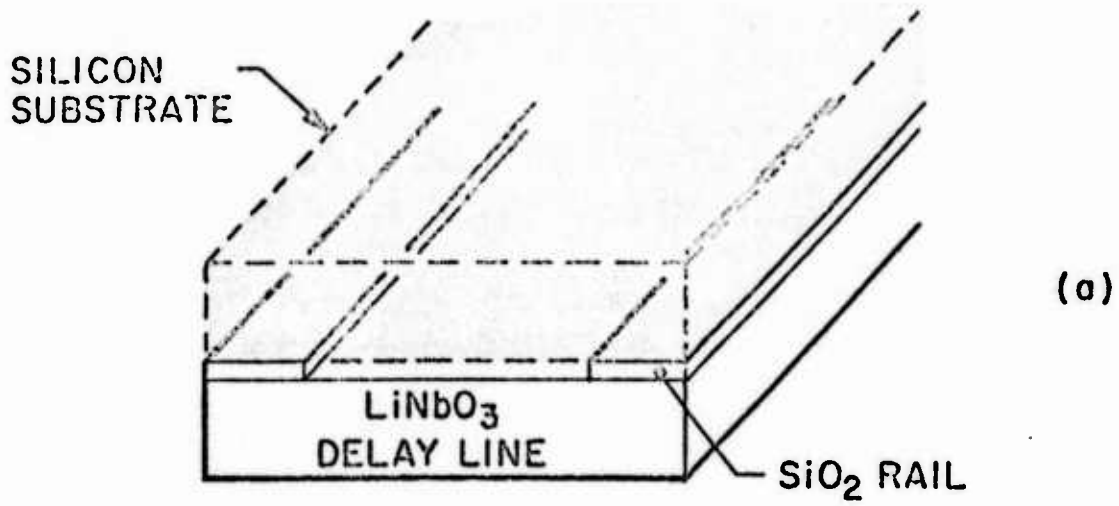


Fig. 1. Methods of defining the convolver airgap. (a) SiO₂ rails; (b) posts; (c) narrow rails

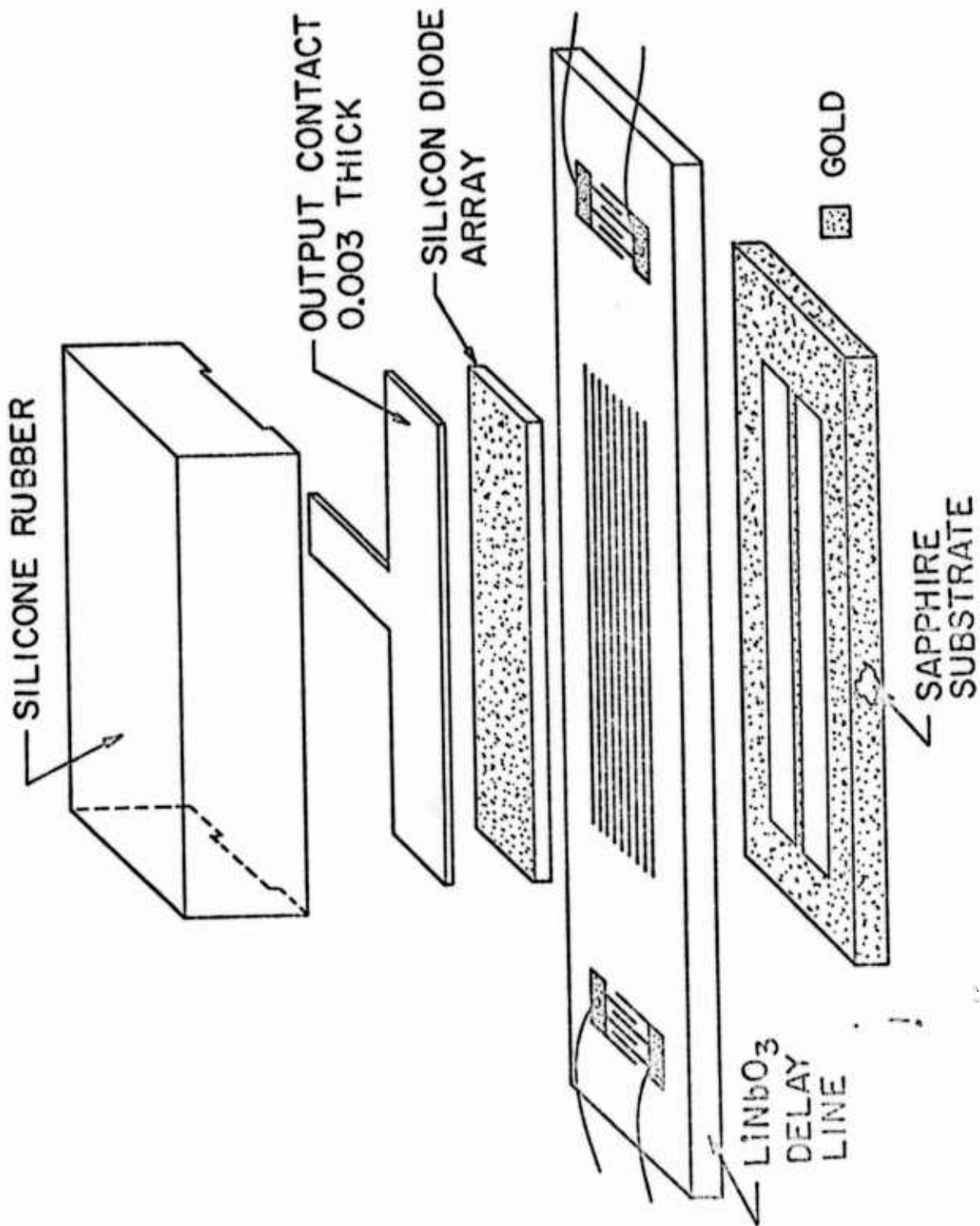
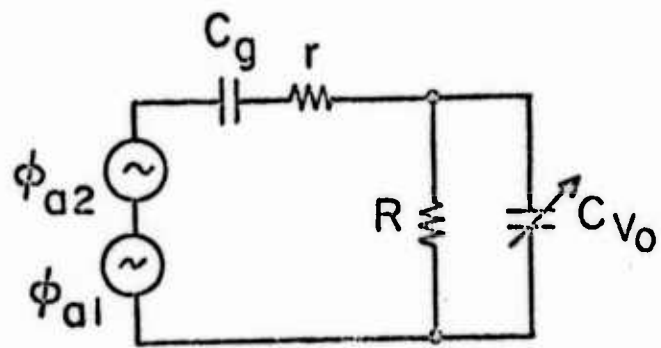
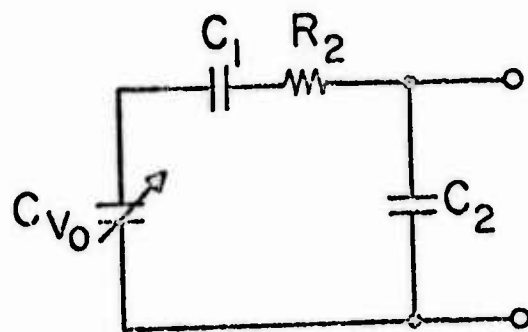


Fig. 2. The convolver assembly.



(a)



(b)

Fig. 3. Convolver equivalent circuits: (a) input; (b) output

APPENDIX

CORRELATION WITH THE STORAGE CONVOLVER

by

P. G. Borden and G. S. Kino

Preprint

G. L. Report No. 2586

June 1976

Rev.

August 1976

NSF Grant ENG75-18681

and

Contract N00014-75-C-0632

submitted to

Applied Physics Letters

Edward L. Ginzton Laboratory
W. W. Hansen Laboratories of Physics
Stanford University
Stanford, California

CORRELATION WITH THE STORAGE CONVOLVER*

by

P. G. Borden and G. S. Kino

Stanford University
Stanford, California

94305

Abstract

A p-n junction type storage convolver has been used to correlate FM chirps with time-bandwidth products of approximately 90 , and to correlate echoes from an acoustic A-scan system which have been badly distorted by the source transducer.

*This work was supported partially by the National Science Foundation under Grant NSF ENG75-18681, and partially by the Office of Naval Research under Contract N00014-75-C-0632.

CORRELATION WITH THE STORAGE CONVOLVER

Recently, it has been suggested by Stern¹, that the storage correlator based on the acoustic surface wave convolver could be used to remove the inherent distortions in a radar system. When a radar emits a coded waveform and the reflected echo is correlated with the original reference code, good correlation is only obtained if the emitted waveform is not distorted by the system or the medium through which it passes. Thus, with the development of more sophisticated systems with large time-bandwidth products, the requirement on the radar system itself becomes very severe, as do the requirements on the lack of signal distortion along the path of the radar beam. Similar problems occur in acoustic pulse echo systems used in medical imaging, sonar, and nondestructive testing, where distortions due to the acoustic transducers and the medium itself can be severe.

In this paper we describe an experiment using a storage correlator to remove the worst errors of this type. We employed an acoustic transducer to emit an FM chirp which was reflected from a plastic plate in a water tank. The reflected echo was used as a reference stored in the storage correlator. A later echo was then correlated with the reference echo. Thus, both echoes suffered the same distortion and a reasonable correlation peak could be obtained.

Our experiment employed the v-groove isolated p-n junction mesa diode array airgap convolver described by Joly.² When this device is used as a storage correlator, the v-groove isolation technique allows a small separation between diodes ($4 \mu\text{m}$) without sacrificing isolation between adjacent diodes.

Several modes of storage correlator operation have been previously described.^{3,4,5,6} In the present case, a charge pattern is written into the

diode array through the nonlinear interaction of an rf signal applied to the diode array top plate (T) and the electric fields associated with a short acoustic pulse injected on the interdigital transducer (L) which travels along the delay line, as illustrated schematically in Fig. 2. After the storage interval, by applying an rf signal to the top plate (T), the convolution of this signal with the stored signal is obtained at the original input port, and the correlation of the two signals at the other acoustic port. In the present case, one transducer is used for a short input storage pulse, and the other for readout. In general, the output will be the correlation of the second top plate input signal and the stored signal. Typical input levels are 25 dBm at the acoustic port, and 60 volts p-p at 93 MHz between the top plate and ground. The half-height storage time is 8 msec.

In a demonstration of high frequency broadband linear FM chirp compression, the acoustic input was a 50 nsec 93 MHz pulse and the top plate signals were two 6 μ sec long 15 MHz (90 to 105 MHz) chirps spaced 200 μ sec apart. The chirp bandwidth was limited by the bandwidth of the top plate matching network; the length limit was the acoustic length of the diode array.

Figure 1 shows the correlation peak obtained. The full width at half maximum is less than 80 nsec, corresponding to a compression ratio of better than 75. This favorably compares to the time-bandwidth product of $(6 \mu\text{sec}) \times (15 \text{ MHz}) = 90$.

A practical application of this pulse compression technique is the elimination of resolution deterioration due to poor transducer response in a pulse echo system. To demonstrate this, a 3.25 MHz center

frequency, 2.5 MHz bandwidth PZT transducer was placed 16 cm from a plastic block in a water tank, as illustrated in Fig. 2. The transducer was pulsed with a constant amplitude linear FM chirp. A 6 μ sec long, 2.5 MHz segment of the first reflected pulse from the plastic block was gated, mixed with 98 MHz, and stored in the correlator (see Figure 2). The gate to the top plate was then reopened to allow correlation of a second echo pulse with the stored first reflected pulse. This second echo was the triple transit signal returning from the plastic block, reflected from the transducer face, and reflected a second time from the plastic block. The second echo was obtained approximately 210 μ sec after the first one used as the stored reference.

Figures 3a,b show the correlation peak and, for comparison, the impulse response of the transducer. The width of the correlation peak corresponds to a compression ratio of 9, compared with the TB limit of 15.

The same experiment was tried a second time with a poor quality transducer that exhibited severe ringing in its impulse response. Figures 3c,d, and e show the first reflected pulse, correlation peak and transducer impulse response respectively. The correlation peak width was essentially the same as that obtained with the original high quality transducer. This indicates that the resolution of the pulse echo system employing the storage correlator is much improved over that which could normally be obtained with a poor quality transducer that severely distorts the original input signal.

ACKNOWLEDGEMENT

The authors wish to thank J. Fraser for his help in setting up the acoustic pulse echo system.

FIGURES

- Fig. 1. Correlation peak obtained with two 6 μ sec long 15 MHz BW chirps.
- Fig. 2. Schematic of the acoustic pulse echo system.
- Fig. 3. Pulse echo experiment results with both good and poor transducers.

REFERENCES

1. E. Stren, Invited Paper, 1975 IEEE Ultrasonics Symposium, Los Angeles (unpublished).
2. R. Joly, this issue.
3. A. Bers and J. H. Cafarella, Appl. Phys. Lett., 25, pp. 133-135, Aug. 1974.
4. H. Hayakawa and G. S. Kino, Appl. Phys. Lett., 25, pp. 178-180, Aug. 1974.
5. K. A. Ingebrigtsen, R. A. Cohen, and R. W. Mountain, Appl. Phys. Lett., 26, pp. 596-598, June 1975.
6. C. Maerfeld, Ph. Defranould, and P. Tournois, Appl. Phys. Lett., 27, pp. 577-578, 1975.

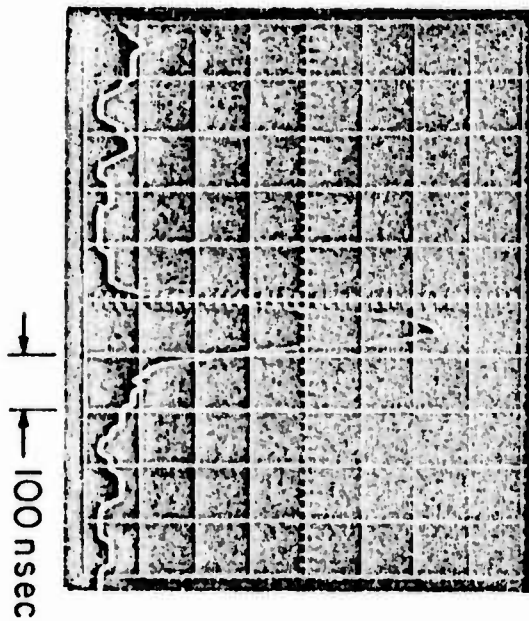


Fig. 1. Correlation peak obtained with two $6\mu\text{sec}$ long 15 MHz BW chirps.

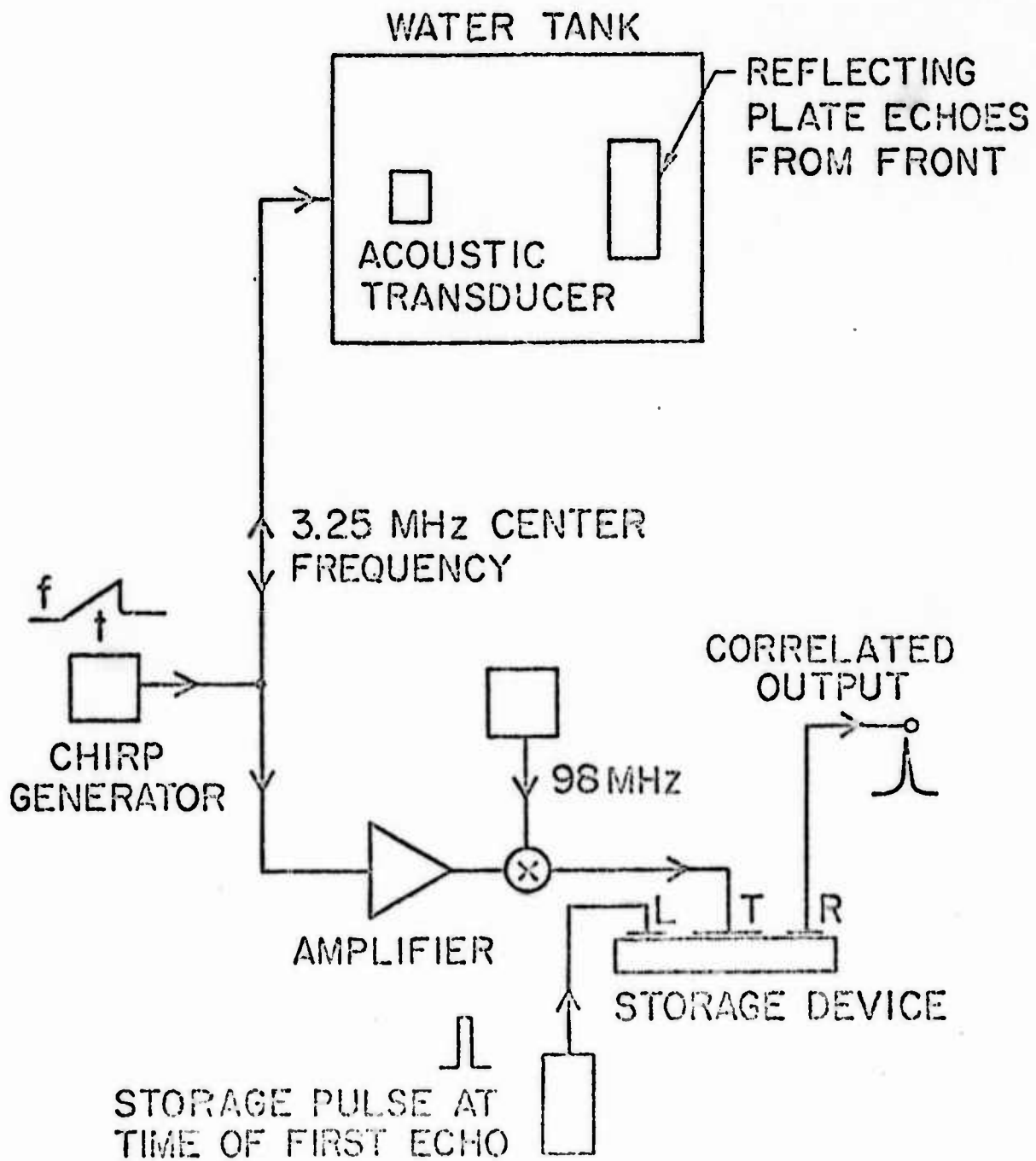
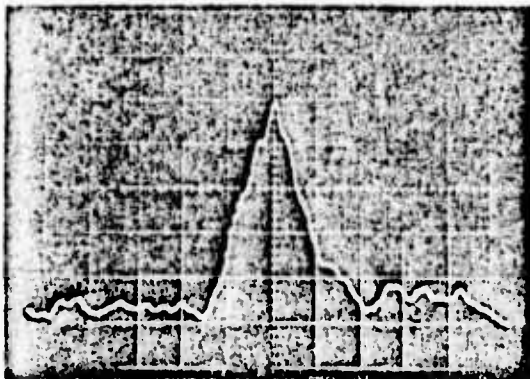


Fig. 2. Schematic of the acoustic pulse echo system.

GOOD TRANSDUCER

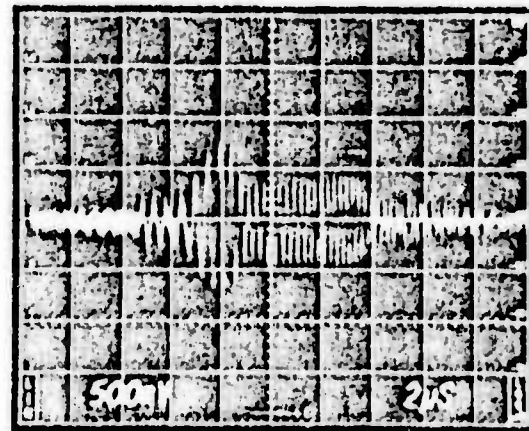
POOR TRANSDUCER

(a) CORRELATION PEAK



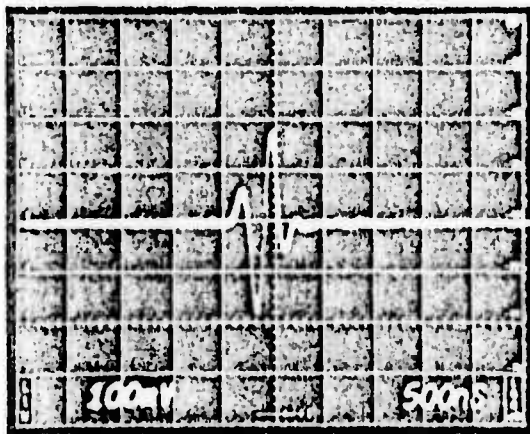
400 nsec/div

(c) FIRST REFLECTION

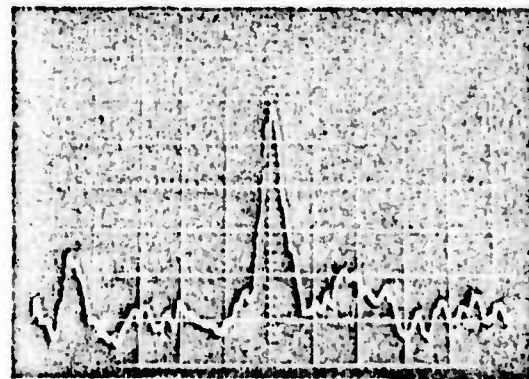


2 MHz 4.5 MHz

(b) IMPULSE RESPONSE



(d) CORRELATION PEAK



1 μsec/div

(e) IMPULSE RESPONSE

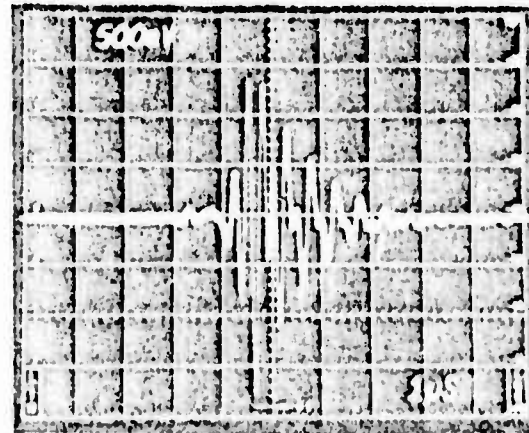


Fig. 3. Pulse echo experiment results with both good and poor transducers.